Supplementary Information

Characterization of SARS-CoV-2 Omicron BA.2.75 clinical isolates

Ryuta Uraki[1,2,14], Shun Iida[3,14], Peter J. Halfmann[4,14], Seiya Yamayoshi[1,2,14], Yuichiro Hirata[3], Kiyoko Iwatsuki-Horimoto[1], Maki Kiso[1], Mutsumi Ito[1], Yuri Furusawa[1,2], Hiroshi Ueki[1,2], Yuko Sakai-Tagawa[1], Makoto Kuroda[4], Tadashi Maemura[4], Taksoo Kim[4], Sohtaro Mine[3], Noriko Iwamoto[5], Rong Li[6], Yanan Liu[6], Deanna Larson[6], Shuetsu Fukushi[7], Shinji Watanabe[8], Ken Maeda[9], Zhongde Wang[6], Norio Ohmagari[5], James Theiler[10], Will Fischer[11,12], Bette Korber[11,12]¶, Masaki Imai[1,2]¶, Tadaki Suzuki[3]¶, and Yoshihiro Kawaoka[1,2,4,13]¶

[1]Division of Virology, Institute of Medical Science, University of Tokyo, Tokyo 108-8639, Japan

[2]The Research Center for Global Viral Diseases, National Center for Global Health and Medicine Research Institute, Tokyo 162-8655, Japan

[3]Department of Pathology, National Institute of Infectious Diseases, Tokyo 162-8640, Japan

[4]Influenza Research Institute, Department of Pathobiological Sciences, School of Veterinary Medicine, University of Wisconsin-Madison, Madison, WI 53711, USA

[5]Disease Control and Prevention Center, National Center for Global Health and Medicine Hospital, Tokyo 162-8655, Japan

[6]Department of Animal, Dairy, and Veterinary Sciences, College of Agriculture and Applied Sciences, Utah State University, Logan, UT 84322, USA

[7]Department of Virology 1, National Institute of Infectious Diseases, Musashimurayama, Tokyo 208-0011, Japan

[8]Center for Influenza and Respiratory Virus Research, National Institute of Infectious Diseases, Musashimurayama, Tokyo 208-0011, Japan

[9]Department of Veterinary Science, National Institute of Infectious Diseases, Tokyo 162-8640, Japan

[10]Space Data Science and Systems, Los Alamos National Laboratory, Los Alamos, NM 87545, USA

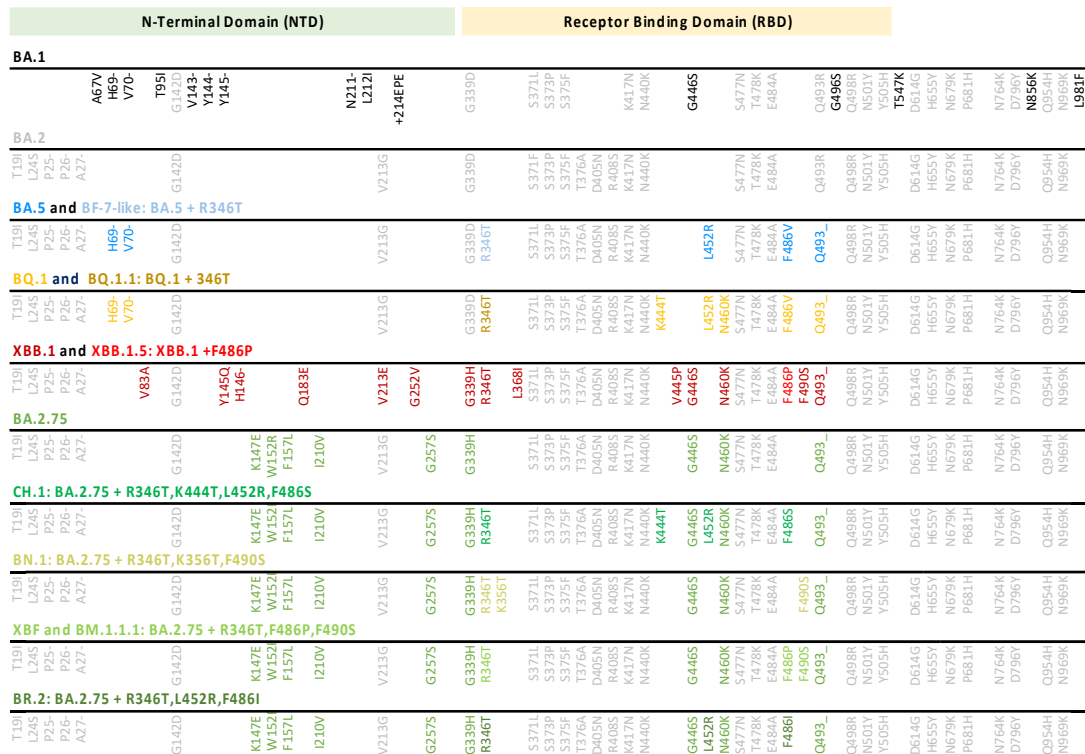[11]Theoretical Biology and Biophysics, Los Alamos National Laboratory, Los Alamos, NM 87545, USA

[12]New Mexico Consortium, Los Alamos, NM 87545, USA

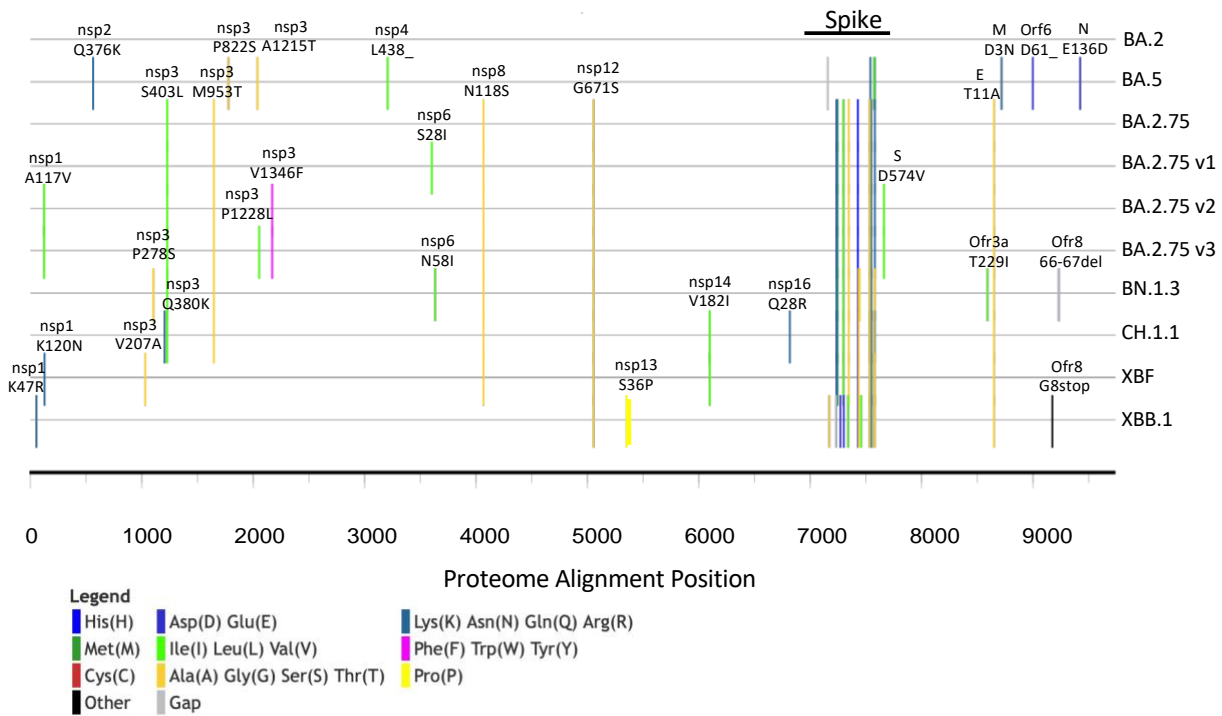[13]The University of Tokyo, Pandemic Preparedness, Infection and Advanced Research Center, Tokyo 162-8655, Japan

[14]These authors contributed equally

¶Corresponding authors

Supplementary Figure 1. Amino acid differences between representative forms of recently emerged Omicron variants.

a, Amino acid differences in the Spike of commonly circulating Omicron variants. BA.1 was rapidly globally replaced by BA.2; the most common form of BA.2 serves as the reference. Spike amino acid differences between the ancestral strain WIV04/2019 (Pango lineage A; Accession ID: EPI_ISL_402124 (https://gisaid.org/wiv04/))

and the baseline form of BA.2 are shown in grey. When other Omicron variants share spike BA.2-defining mutations in a given position, they are noted in grey. When they differ, the amino acid change is highlighted in the color assigned to each variant (the same color as used in **Figure 1**). Representative forms of the variants that are currently commonly circulating are shown: BA.5, BF-7-like lineages that resemble BA.5 lineages with the addition of R346T, and BQ.1 and BQ.1.1 sublineages; XBB sublineages including XBB.1.5; and several common BA.2.75 sublineages. Four representative forms of currently circulating BA.2.75 sublineage spikes are highlighted in shades of green. The recombinant lineage XBF is included here because it carries a BA.2.75 lineage Spike. Deletions are indicated by a dash (-), insertions by a plus sign (e.g., +214EPE means a three amino acid insertion of EPE after position 214). Reversions from BA.2 to the ancestral form are indicated by an underscore (_). b, Highlighting amino acid differences between BA.2, BA.5, and BA.2.75 and examples of BA.2.75 variants throughout the full proteome. Only amino differences from the most representative form of BA.2 are shown, illustrated as a tick mark. The grey line represents the full proteome. All changes in the most common forms of BA.5 and BA.2.75 relative to BA.2 are noted, as these are candidates for contributing to a selective advantage for BA.5 over BA.2, and for BA.2.75 over BA.5 and BA.2. Details for the amino acid differences are shown in part a. Amino acids that are distinctive in the three BA.2.75 variants studied in this paper are highlighted, BA.2.75 V1–V3, as well as several sublineages of BA.2.75 that have persisted into 2023. Full-length representative forms of Pango lineages are defined as the most common circulating form of a given Pango lineage.

Countries	Number of CH.1 sequences	Number of other sequences	Total number of seugences	CH.1/Total (%)	Number of days sampled	One sided p-value, CH.1.1 increasing
Australia	671	19039	19710	3.4	82	0.00249
Austria	373	30546	30919	1.21	82	0.00249
Belgium	94	3676	3770	2.49	81	0.00249
Brunei	15	755	770	1.95	61	0.00249
Cambodia	20	176	196	10.2	54	0.00249
Canada	215	32532	32747	0.66	83	0.00249
Chile	18	2908	2926	0.62	80	0.00498
Czech Republic	12	1123	1135	1.06	71	0.00249
Denmark	1200	32196	33396	3.59	83	0.00249
Finland	33	2571	2604	1.27	73	0.00249
France	172	24834	25006	0.69	76	0.00249
Germany	426	38287	38713	1.1	80	0.00249
Greece	77	2977	3054	2.52	56	0.04478
Hong-Kong	139	576	715	19.44	72	0.00249
Iceland	51	1130	1181	4.32	81	0.00249
India	27	1362	1389	1.94	76	0.00498
Indonesia	39	5153	5192	0.75	77	0.00249
Ireland	618	4652	5270	11.73	85	0.00249
Israel	121	5533	5654	2.14	64	0.00249
Italy	92	9976	10068	0.91	83	0.00249
Japan	704	65446	66150	1.06	87	0.00249
Liechtenstein	13	137	150	8.67	55	0.99502
Lithuania	28	499	527	5.31	35	0.00249
Luxembourg	64	3673	3737	1.71	79	0.00249
Malaysia	94	3633	3727	2.52	79	0.00249
Netherlands	376	8666	9042	4.16	80	0.00249
New Zealand	726	4245	4971	14.6	53	0.00249
Norway	15	1232	1247	1.2	70	0.26617
Peru	55	4731	4786	1.15	63	0.00249
Poland	17	810	827	2.06	74	0.00498
Portugal	54	1592	1646	3.28	72	0.00249
Singapore	158	3692	3850	4.1	82	0.00249
Slovenia	66	3901	3967	1.66	77	0.00249
Solomon Islands	35	50	85	41.18	22	0.47264
South Korea	266	15983	16249	1.64	73	0.00249
Spain	162	8626	8788	1.84	83	0.00249
Sweden	360	10813	11173	3.22	79	0.00249
Switzerland	69	4628	4697	1.47	79	0.00249
Thailand	136	1714	1850	7.35	65	0.02488
USA	1352	194535	195887	0.69	87	0.00249
United Kingdom	6665	43545	50210	13.27	83	0.00249

Range of dates considered: 2022-10-29 - 2023-01-27

There were 15,938 CH.1 sequences that matched the search term: CA.7, CH.1, CH.1.1, CH.1.1.1, CH.1.1.2, CV.1

CH.1 and CH.1.1 lineages were increasingly sampled in 38/41 countries where it had been sampled $\geq$ 10 times. They have the consensus form BA.2.75 +[R346T,K444T,L452R,F486S]
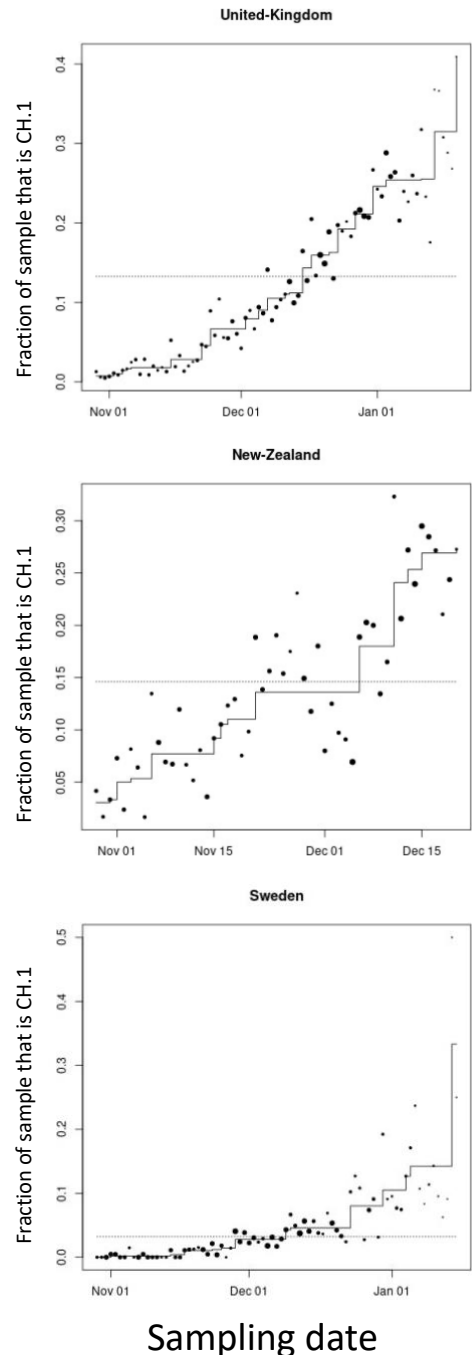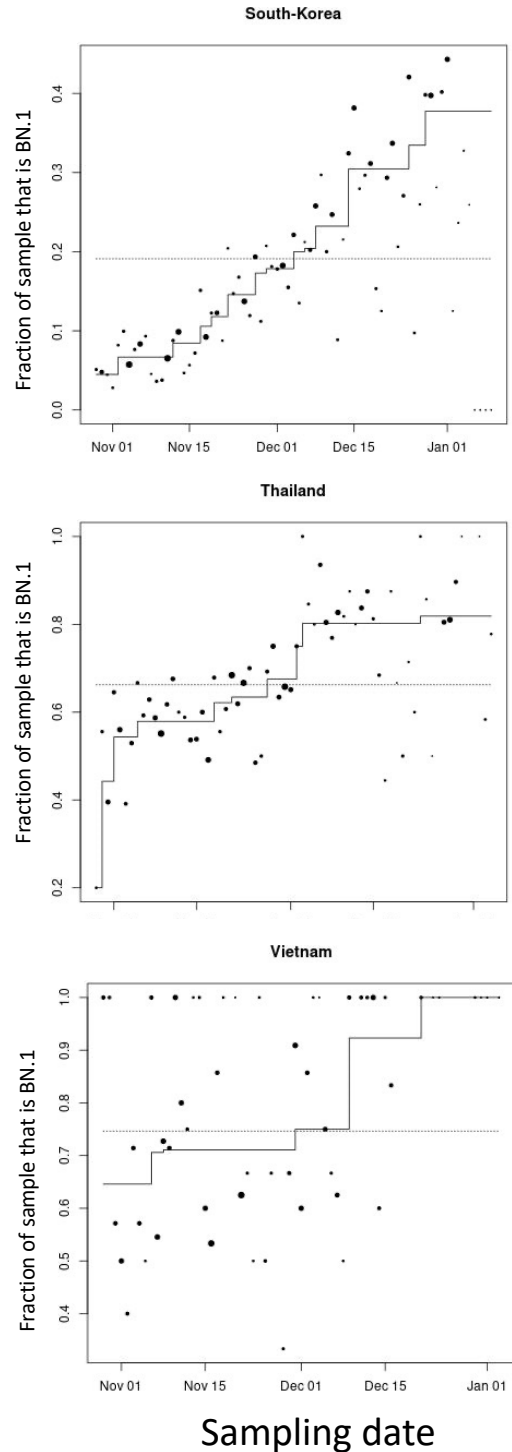
Supplementary Figure 2. Isotonic regression analysis showing BA.2.75 sublineage CH.1 and related lineages are increasingly sampled over time in countries where they have become established.

The table provides summary statistics for all countries where CH.1 sequences have been sampled at least 10 times with a sampling date between Oct 29, 2022 and Jan 27, 2023. Three examples of the data over time are plotted to illustrate the increasing frequency of CH.1 sampling. The proportion of CH.1-related lineages in the total sample (y-axis) is calculated each day samples are available (x-axis). The size of the dot reflects the relative sample size on a given day. The *p*-value is calculated based on a one-sided resampling test with 400

randomizations. The results can be updated online using the Isotonic Regression tool at cov.lanl.gov. (https://cov.lanl.gov/content/sequence/ISORG/pango_isorg.html)[26]. CH.1 and BN.1 (Supplementary Fig. 3) related forms were chosen for display because they are currently the mostly commonly sampled BA.2.75 sublineages.

| Countries	Number of BN.1 sequences	Number of other sequences	Total number of seugences	BN.1/Total (%)	Number of days sampled	One sided p-value BN.1 increasing
Australia	1973	17737	19710	10.01	82	0.00249
Austria	720	30199	30919	2.33	82	0.00249
Belgium	125	3645	3770	3.32	81	0.1393
Brazil	78	9367	9445	0.83	70	0.00249
Brunei	43	727	770	5.58	61	0.33831
Cambodia	122	74	196	62.24	54	0.26617
Canada	452	32295	32747	1.38	83	0.00249
Chile	28	2898	2926	0.96	80	0.81841
China	40	6215	6255	0.64	83	0.86567
Colombia	41	1080	1121	3.66	57	0.45522
Croatia	34	1268	1302	2.61	55	0.00249
Czech Republic	78	1057	1135	6.87	71	0.00249
Denmark	4151	29245	33396	12.43	83	0.00249
Finland	36	2568	2604	1.38	73	0.35572
France	619	24387	25006	2.48	76	0.00249
Georgia	53	86	139	38.13	32	0.00249
Germany	2001	36712	38713	5.17	80	0.00249
Greece	99	2955	3054	3.24	56	0.00249
Hong-Kong	23	692	715	3.22	72	0.00249
Iceland	177	1004	1181	14.99	81	0.28856
India	88	1301	1389	6.34	76	0.6194
Indonesia	240	4952	5192	4.62	77	0.83831
Iran	24	84	108	22.22	32	0.45274
Ireland	315	4955	5270	5.98	85	0.00249
Israel	287	5367	5654	5.08	64	0.01741
Italy	237	9831	10068	2.35	83	0.00249
Japan	3582	62568	66150	5.41	87	0.00249
Kenya	10	226	236	4.24	39	0.53483
Laos	25	16	41	60.98	24	0.00249
Latvia	69	1126	1195	5.77	46	0.00249
Liechtenstein	10	140	150	6.67	55	0.75871
Lithuania	53	474	527	10.06	35	0.00249
Luxembourg	145	3592	3737	3.88	79	0.00249
Malaysia	454	3273	3727	12.18	79	0.76368
Mauritius	206	231	437	47.14	33	0.00249
Mexico	59	1781	1840	3.21	59	0.28358
Moldova	10	36	46	21.74	28	0.70647
Netherlands	514	8528	9042	5.68	80	0.0199
New Zealand	220	4751	4971	4.43	53	0.00249
Norway	33	1214	1247	2.65	70	0.39801
Peru	35	4751	4786	0.73	63	0.47761
Poland	35	792	827	4.23	74	0.00249
Portugal	51	1595	1646	3.1	72	0.00995
Puerto-Rico	31	899	930	3.33	49	0.64925
Romania	28	178	206	13.59	50	0.16915
Russia	90	4103	4193	2.15	50	0.00249
Singapore	358	3492	3850	9.3	82	0.00249
Slovakia	13	427	440	2.95	62	0.18657
Slovenia	107	3860	3967	2.7	77	0.00249
South-Africa	11	1096	1107	0.99	75	0.22139
South-Korea	3104	13145	16249	19.1	73	0.00249
Spain	159	8629	8788	1.81	83	0.96269
Sweden	401	10772	11173	3.59	79	increasing
Switzerland	176	4521	4697	3.75	79	0.15423
Thailand	1225	625	1850	66.22	65	0.00249
Trinidad and Toba	75	270	345	21.74	75	0.00249
USA	5522	190365	195887	2.82	87	0.00249
United Kingdom	3250	46960	50210	6.47	83	0.00249
Vietnam	215	73	288	74.65	53	0.00498

Range of dates considered: 2022-10-29 - 2023-01-27

There were 32,568 BN.1 sequences that matched the search term: BN.1, BN.1.1, BN.1.1.1, BN.1.2, BN.1.2.1, BN.1.3, BN.1.3.1, BN.1.4, BN.1.5, BN.1.6, BN.1.7, BN.1.8, BN.1.9

BN.1 and BN.1.1 lineages were increasingly sampled in 35/59 countries where they had been sampled $\geq$ 10 times. They have the consensus form BA.2.75 +[R346T,K356T,F490S]

Supplementary Figure 3. Isotonic regression analysis showing BA.2.75 sublineage BN.1 and related forms are increasingly sampled over time in countries where they have become established.

This figure follows the format of Supplementary Fig. 2, but here the table provides summary statistics for all countries where BN.1 sequences have been sampled at least 10 times between Oct 29, 2022 and Jan 27, 2023. As before, three examples are plotted to illustrate the increasing frequency of BN.1 sampling, and the proportion of BN.1-related lineages in the total sample (y-axis) is calculated each day samples are available (x-axis). The size of the dot reflects the relative sample size on a given day. The p-value is calculated based on a one-sided resampling test with 400 randomizations. The results can be updated online using the Isotonic Regression tool at cov.lanl.gov. (https://cov.lanl.gov/content/sequence/ISORG/pango_isorg.html)[26]. As noted above, CH.1 and BN.1 (Supplementary Fig. 2) were highlighted because they are currently the mostly commonly sampled BA.2.75 sublineages.
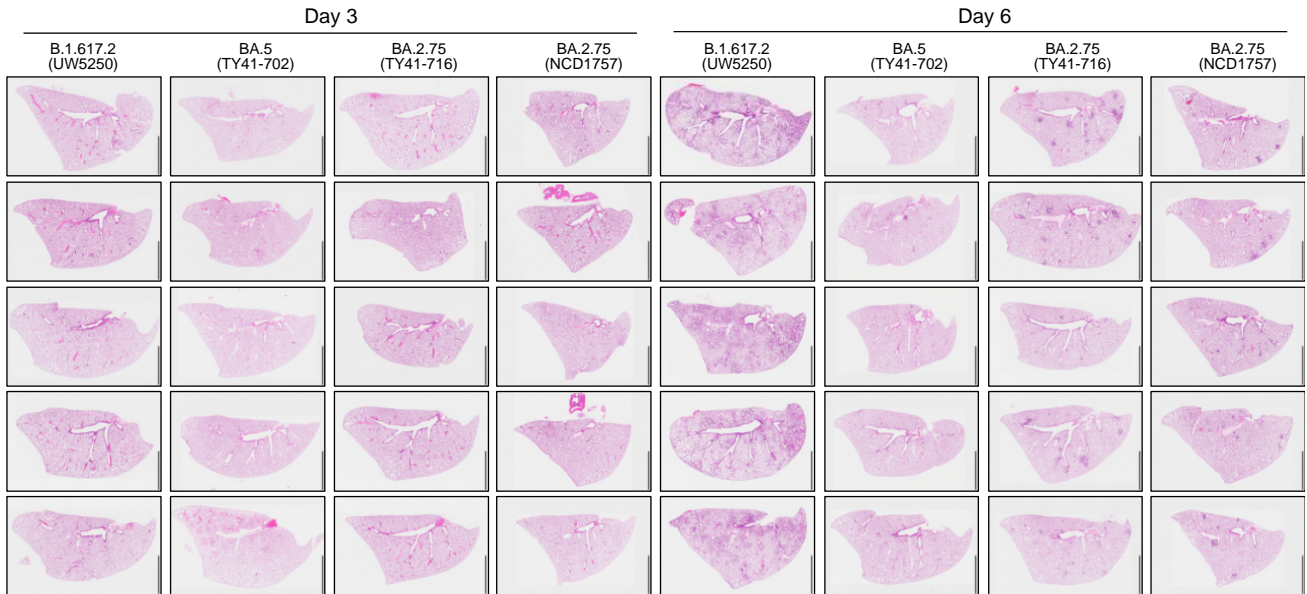
Supplementary Figure 4. Semi-macroscopic images of the lungs of hamsters inoculated with SARS-CoV-2.

Wild-type Syrian hamsters ($n = 5$, per group) were inoculated with 10^5 PFU of BA.2.75 (TY41-716), BA.2.75 (NCD1757), BA.5 (TY41-702), or B.1.617.2 (UW5250) and sacrificed at 3 or 6 dpi for histopathological examinations. Semi-macroscopic images (hematoxylin and eosin staining) of the lungs from all animals examined are shown. Scale bars, 5 mm. Data are from one experiment.

a SARS-CoV-2 infectious virus titers

Day 5 WT hamster
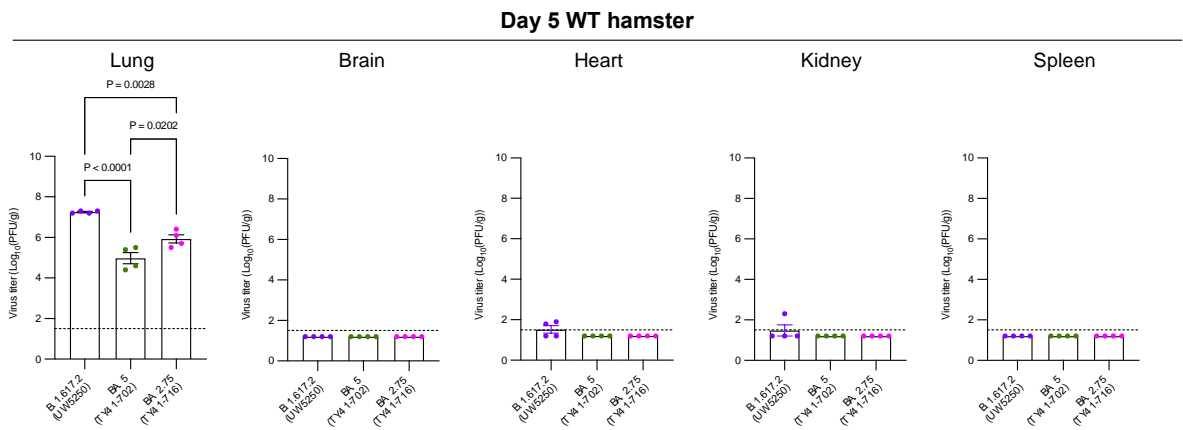
b SARS-CoV-2 N sgRNA levels

Day 5 WT hamster
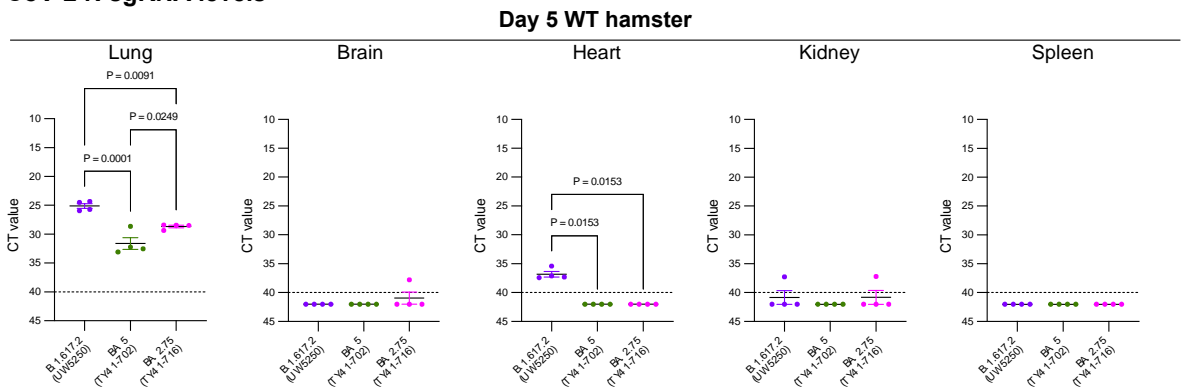
Supplementary Figure 5. Viral replication in lungs and extrapulmonary organs of wild-type hamsters inoculated with BA.2.75.

Wild-type Syrian hamsters ($n = 4$) were inoculated with 10^5 PFU of BA.5 (TY41-702), BA.2.75 (TY41-716), or B.1.617.2 (UW5250). Viral titers (**a**) and levels of subgenomic RNA (sgRNA) targeting the N gene (**b**) in the lungs, brain, heart, kidneys, and spleen of infected animals were measured at 5 dpi. Viral titers and sgRNA levels in the organs were determined by performing plaque assays and quantitative real-time PCR, respectively. Data are means ± s.e.m. Points represent data from individual hamsters; the lower limit of detection is indicated by the horizontal dashed line. Data were analyzed with the Kruskal–Wallis test with Dunn's multiple comparisons (titers and sgRNA levels in the extrapulmonary organs of infected hamsters) or a one-way ANOVA with Tukey's multiple comparisons test (titers and sgRNA levels in the lungs of infected hamsters).
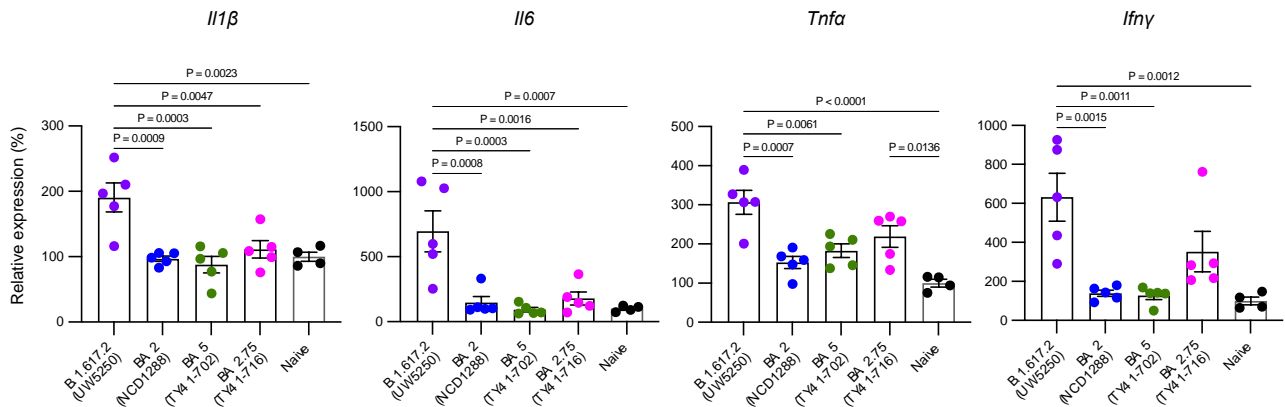
Supplementary Figure 6. Host responses in the lungs of wild-type hamsters infected with BA.2.75.
Wild-type Syrian hamsters (n = 5) were intranasally inoculated with 10^5 PFU in 30 μL of BA.2 (NCD1288), BA.5 (TY41-702), BA.2.75 (TY41-716), or B.1.617.2 (UW5250). Pro-inflammatory cytokine gene expression levels (*Il1β*, *Il6*, *Tnfα*, and *Ifnγ*) in the lungs of the infected hamsters were assessed at 3 dpi (infected hamsters, n = 5; naïve uninfected hamsters, n = 4). Vertical bars show the mean ± s.e.m. Points indicate data from individual mice. Data were analyzed by using a one-way ANOVA with Tukey's multiple comparisons test. Data are from one experiment.